

Dalton Transactions

Accepted Manuscript



This article can be cited before page numbers have been issued, to do this please use: J. Zhang, Y. Wang, N. Luo, K. Wu, Z. Chen and G. Yin, *Dalton Trans.*, 2015, DOI: 10.1039/C5DT00804B.



This is an *Accepted Manuscript*, which has been through the Royal Society of Chemistry peer review process and has been accepted for publication.

Accepted Manuscripts are published online shortly after acceptance, before technical editing, formatting and proof reading. Using this free service, authors can make their results available to the community, in citable form, before we publish the edited article. We will replace this *Accepted Manuscript* with the edited and formatted *Advance Article* as soon as it is available.

You can find more information about *Accepted Manuscripts* in the [Information for Authors](#).

Please note that technical editing may introduce minor changes to the text and/or graphics, which may alter content. The journal's standard [Terms & Conditions](#) and the [Ethical guidelines](#) still apply. In no event shall the Royal Society of Chemistry be held responsible for any errors or omissions in this *Accepted Manuscript* or any consequences arising from the use of any information it contains.

ARTICLE

Redox inactive metal ions triggered N-dealkylation by iron catalyst with dioxygen activation: a lesson from lipoxygenases

Cite this: DOI: 10.1039/x0xx00000x

Received 00th January 2012,
Accepted 00th January 2012

DOI: 10.1039/x0xx00000x

www.rsc.org/Jisheng Zhang, Yujuan Wang, Nengchao Luo, Zhuqi Chen, Kangbing Wu,
Guochuan Yin*

Utilization of dioxygen as the terminal oxidant at ambient temperature is always a challenge in redox chemistry, because it is hard to oxidize the stable redox metal ions like iron(III) to its high oxidation state to initialize the catalytic cycle. Inspired by the dioxygenation and co-oxidase activity of lipoxygenases, herein, we introduce an alternative protocol to activate the sluggish iron(III) species with non-redox metal ions, which can promote its oxidizing power to facilitate substrate oxidation with dioxygen, thus initialize the catalytic cycle. In oxidations of *N,N*-dimethylaniline and its analogues, adding Zn(OTf)₂ to [Fe(TPA)Cl₂]Cl catalyst can trigger the amine oxidation with dioxygen, whereas [Fe(TPA)Cl₂]Cl alone is very sluggish. In stoichiometric oxidations, it has also confirmed that the presence of Zn(OTf)₂ can apparently improve the electron transfer capability of the [Fe(TPA)Cl₂]Cl complex. Experiments using different type of substrates as trapping reagent disclosed that the iron(IV) species does not occur in the catalytic cycle, suggesting that oxidation of amines is initialized by electron transfer rather than hydrogen abstraction. Combined experiments from UV-Vis, high resolution mass spectrometry, electrochemistry, EPR and oxidation kinetics support that the improved electron transfer ability of iron(III) species originates from its interaction with added Lewis acids like Zn²⁺ through plausible chloride or OTf bridge, which has promoted the redox potential of iron(III) species. The amine oxidation mechanism was also discussed based on available data, which resembles the co-oxidase activity of lipoxygenases in oxidative dealkylation of xenobiotic metabolisms where external electron donor is not essential for dioxygen activation.

Introduction

Active metal intermediates play the crucial roles in versatile biological and chemical oxidation events;¹ however, dioxygen activation is still a long challenge in redox metal ions mediated catalytic oxidations at ambient temperature.² For example, iron(III) cation is usually the most stable form of the iron ions in solution at ambient temperatures, and it is seldom to report that, in the absence of co-reductant, dioxygen can oxidize it to the iron(IV) form which is the active intermediate in a variety of oxidation processes.³ Alternatively, versatile activated oxidants such as hydrogen peroxide, iodosylbenzene and peracetic acid were employed as the terminal oxidants for these redox metal ions mediated catalytic oxidations.⁴ On the other hand, in nature, dioxygen is the solely terminal oxidant employed by redox enzymes in versatile biological metabolism and synthesis.⁵ To achieve efficient dioxygen activation, for example in P450 enzyme, one electron from electron transfer chain needs to be transferred to the Fe^{III}(Porphyrin) to form the reduced Fe^{II}(Porphyrin) intermediate. The unstable

Fe^{II}(Porphyrin) next feasibly activates dioxygen to generate a peroxy iron(III) intermediate (Porphyrin)Fe^{III}-OO[•], which initializes the catalytic cycle.⁶ Similar dioxygen activation also happens in many non-heme enzymes mediated oxidations.⁷ However, there exist exceptions. For example, lipoxygenases do not need an electron transfer chain for dioxygen activation. In lipoxygenases, the active intermediate has a Fe(III)-OH functional group which is capable of abstracting hydrogen atom from unsaturated fatty acid to generate a substrate radical. After isomerization, this substrate radical traps dioxygen to form a peroxy radical intermediate which next oxidizes the reduced iron(II) species back to the active iron(III) species, and releases the lipid hydroperoxide product.⁸ In particular, the generated peroxy radical intermediate and/or hydroperoxide products serve as oxidants in the co-oxidase activity of lipoxygenases for versatile xenobiotic metabolisms.⁹ While, in chemical oxidations, there does not exist such an electron transfer chain to deliver electron to the stable redox metal ions for generating the reduced, unstable intermediate which can activate dioxygen

under ambient conditions, and these normally stable redox metal ions like iron(III) are also not able to trigger an efficient catalytic oxidation with dioxygen at ambient temperature.

In heterogeneous catalysis using dioxygen at elevated temperature, in addition to the redox metal ions, there exist certain non-redox metal ions as additives to modify the reactivity and stability of the catalysts.¹⁰ Similar redox inactive metal ions also occur in redox enzymes, for example, Ca^{2+} in photosystem II.¹¹ Although their roles are not fully understood yet, it has inspired the chemists to address their mechanisms using synthetic models. Lau first observed that Al^{3+} and BF_3 as Lewis acid may accelerate stoichiometric oxidation of alkane by MnO_4^- ;¹² Collins found that Mg^{2+} , Zn^{2+} and Sc^{3+} can accelerate triphenylphosphine oxygenation by their $\text{Mn}^{\text{V}}(\text{TAML})$ analog.¹³ Recently, Nam and Fukuzumi extensively investigated Lewis acid accelerated stoichiometric oxidations of sulfide with iron(IV) and manganese(IV) oxo complexes;¹⁴ Goldberg also found that adding Zn^{2+} or organic Lewis acid can cause the valence tautomerization of their manganese(V) oxo porphyrinoid complex to the manganese(IV) oxo porphyrinoid π radical intermediate, and accelerate its rates in both hydrogen abstraction and electron transfer.¹⁵ These acceleration effects were generally attributed to the ligation of Lewis acid to the metal oxo functional group, which leads to the increase of their redox potentials. The linkage of Lewis acid with metal oxo was evidenced by the X-ray crystal structure of Sc^{3+} bound non-heme iron(IV) complex.¹⁶ Notably, Borovik reported that Ca^{2+} can promote dioxygen activation by their manganese(II) or iron(II) complexes;¹⁷ we also found that the presence of Ca^{2+} and Cl^- can synergistically affect the redox potentials of manganese complex, thus modify its catalytic reactivity.¹⁸ Most recently, Que found that adding Sc^{3+} can trigger the formation of $\text{Fe}^{\text{IV}}(\text{TMC})$ oxo from $\text{Fe}^{\text{II}}(\text{TMC})$ through dioxygen activation in the presence of BPh_4^- ;¹⁹ Nam and Fukuzumi further revealed that formation of iron(IV) oxo proceeds via Sc^{3+} promoted radical chain autooxidation of iron(II) complex.²⁰ In investigating the reactivity relationship of the active metal oxo, hydroxo and hydroperoxide intermediates in oxidations, we observed that increasing the net charge of an active species through protonation would substantially increase its potential, thus accelerate its electron transfer rate,²¹ which resembles the acceleration behavior of binding Lewis acid to the metal oxo group (Brønsted acid vs Lewis acid). Inspired by these, we explored Al^{3+} promoted Pd(II)-catalyzed benzene hydroxylation through dioxygen activation,²² and manganese(II) complex catalyzed sulfide oxygenation and olefin epoxidation with PhIO and its analogues.²³

Encouraged by these Lewis acid promoted oxidations, we suspect that, in chemical oxidations, although there does not exist an electron transfer chain for reducing normally stable redox metal ions like iron(III) to their unstable form, an essential step for dioxygen activation in many redox enzymes, it is still possible to bind a Lewis acid to these stable redox metal ions, which may promote their capability in oxidizing certain substrate, thus facilitate dioxygen activation and trigger the catalytic cycle. Herein, we demonstrate an early example of

such concept for dioxygen activation in a catalytic process, and we found that, in *N*-dealkylation of amines, adding redox inactive metal ions could substantially accelerate $[\text{Fe}(\text{TPA})\text{Cl}_2]\text{Cl}$ mediated catalytic oxidation with dioxygen, whereas $[\text{Fe}(\text{TPA})\text{Cl}_2]\text{Cl}$ alone is very sluggish.

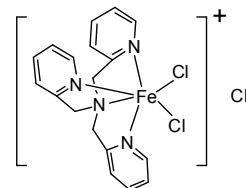


Figure 1. The structure of $[\text{Fe}(\text{TPA})\text{Cl}_2]\text{Cl}$ complex.

Experimental

All chemical reagents are commercially available and used without further purification. Copper(II) trifluoromethanesulfonate ($\text{Cu}(\text{CF}_3\text{SO}_3)_2$), diphenylmethane, *p*-methyl-*N,N*-dimethylaniline, *N,N*,2,4,6-pentamethylaniline, 9,10-dihydroanthracene, *p*-bromo-*N*-methyl aniline and 1,4-cyclohexadiene came from Alfa Aesar; sodium trifluoromethanesulfonate (NaCF_3SO_3), magnesium(II) trifluoromethanesulfonate ($\text{Mg}(\text{CF}_3\text{SO}_3)_2$), scandium trifluoromethanesulfonate ($\text{Sc}(\text{CF}_3\text{SO}_3)_3$) and 4-chlorobenzonitrile were purchased from Aladdin. Other trifluoromethanesulfonates including $\text{Ca}(\text{CF}_3\text{SO}_3)_2$, $\text{Zn}(\text{CF}_3\text{SO}_3)_2$, $\text{Al}(\text{CF}_3\text{SO}_3)_3$, and $\text{Y}(\text{CF}_3\text{SO}_3)_3$ came from Shanghai Dibai Chemical Co. Cyclooctene, *N*-methylaniline and *N*-methylformanilide were purchased from J&K Scientific Ltd. Toluene, thioanisole, *N,N*-dimethylaniline, 4,4-methylenebis-(*N,N*-dimethylaniline), acetonitrile and styrene were purchased from local Sinopharm Chemical Reagent. Xanthene, *p*-cyano-*N,N*-dimethylaniline, *p*-methyl-*N*-methylaniline and 2-(chloromethyl)-pyridine hydrochloride were purchased from HEOWNS. *p*-Bromo-*N,N*-dimethylaniline and 2-picoyl amine were purchased from Accela ChemBio. Ltd. Tris-[(2-pyridyl)methyl]amine (TPA) was synthesized according to the literature.²⁴ The iron complexes including $[\text{Fe}(\text{TPA})\text{Cl}_2]\text{Cl}$, $\text{Fe}(\text{TPA})\text{Cl}_2$ and $\text{Fe}(\text{TPA})(\text{CH}_3\text{CN})_2(\text{OTf})_2$ were also synthesized according to the literatures,²⁵⁻²⁷ and the structure of $[\text{Fe}(\text{TPA})\text{Cl}_2]\text{Cl}$ complex is displayed in Figure 1.

UV-Vis spectra were collected on Analytikjena specord 205 UV-Vis spectrometer. Mass spectra were determined by a VG ZAB HS spectrometer. GC-MS analysis was performed on an Agilent 7890A/5975C spectrometer, and NMR spectra were obtained on a Bruker AV400 spectrometer. Electrochemical data were collected on a CS Corrtest electrochemical workstation equipped with glassy carbon as both working and counter electrodes and saturated calomel as reference electrode. Electrochemical measurements were performed under nitrogen in dry acetonitrile with 0.1 M tetrabutylammonium perchlorate as the supporting electrolyte. Electron paramagnetic resonance (EPR) experiments were conducted at 130 K on a Bruker A200 spectrometer.

General procedure for catalytic N-demethylation by [Fe(TPA)Cl₂]Cl catalyst in the presence of Zn(OTf)₂ In a typical experiment, [Fe(TPA)Cl₂]Cl (4.52 mg, 0.01 mmol), Zn(OTf)₂ (7.26 mg, 0.02 mmol) and *N,N*-dimethylaniline (60.5 mg, 0.5 mmol) were dissolved in 5 mL of acetonitrile in a glass tube, and then the reaction solution was magnetically stirred at 313 K in water bath with dioxygen balloon for 4 h. After the reaction, the products were isolated by silica gel chromatography, and further identified by NMR analysis (NMR data of products are supplied in supporting information). The quantitative analysis was performed by GC with the internal standard method or HPLC using the external standard method, respectively. Control experiments using [Fe(TPA)Cl₂]Cl or Zn(OTf)₂ alone were carried out in parallel. Reactions were performed at least in duplicate, and average data were used in discussion.

General procedure for catalytic kinetics of amine oxidation by [Fe(TPA)Cl₂]Cl in the presence of Zn(OTf)₂ In a typical experiment, [Fe(TPA)Cl₂]Cl (4.52 mg, 0.01 mmol), Zn(OTf)₂ (7.26 mg, 0.02 mmol) and *N,N*-dimethylaniline (60.5 mg, 0.5 mmol) were dissolved in 5 mL of acetonitrile in a glass tube. Then, the reaction solution was magnetically stirred at 313 K in water bath with dioxygen balloon. The product analysis was performed by GC using the internal standard method at set intervals. Control experiments using [Fe(TPA)Cl₂]Cl or Zn(OTf)₂ alone as catalyst were carried out in parallel. *p*-Methyl-*N,N*-dimethylaniline was also used as the substrate for the catalytic kinetic test as described above.

General procedure for stoichiometric oxidation of amine by [Fe(TPA)Cl₂]Cl with Zn(OTf)₂ In a typical experiment, [Fe(TPA)Cl₂]Cl (22.6 mg, 0.05 mmol), Zn(OTf)₂ (36.3 mg, 0.10 mmol) and *N,N*-dimethylaniline (6.05 mg, 0.05 mmol) were dissolved in 5 mL acetonitrile in a glass tube under the argon atmosphere, then the reaction solution was magnetically stirred at 313 K in water bath for 4 h. After the reaction, the product analysis was performed by GC with the internal standard method and HPLC with the external standard method, respectively. Reactions were performed at least in duplicate, and average data were used in discussion. In similar stoichiometric oxidation reaction, [Fe(TPA)Cl₂]Cl (0.05 mM), Zn(OTf)₂ (0.1 mM) and *N,N*-dimethylaniline (0.1 mM) were dissolved in 3 mL of acetonitrile, and then it was recorded by UV-Vis spectrometer at set intervals for stoichiometric oxidation kinetics.

General procedures for hydrogen abstraction, sulfoxidation and epoxidation reactions In a typical experiment, [Fe(TPA)Cl₂]Cl (4.52 mg, 0.01 mmol), Zn(OTf)₂ (7.26 mg, 0.02 mmol) and one of the substrate (0.5 mmol), diphenylmethane, 1,4-cyclohexadiene, styrene, cyclooctene or thioanisole were dissolved in 5 mL of acetonitrile in a glass tube, and then the reaction solution was magnetically stirred at 313 K in water bath with dioxygen balloon for 4 h. After the reaction, the product analysis was performed by GC using the internal standard method. The similar experiments by adding *N,N*-dimethylaniline (0.05 mmol) to above reaction solution were also conducted.

Results and discussion

Lewis acid promoted oxidative N-dealkylation of amines by iron(III) catalyst with dioxygen In present studies, oxidative *N*-demethylation of *N,N*-dimethylaniline (DMA) with iron(III) catalyst was first employed as a model reaction to demonstrate Lewis acid promoted catalytic oxidation through dioxygen activation. In nature, oxidative *N*-dealkylation of amines is an important process in biological metabolisms and DNA repairs, and many redox enzymes including P450 enzymes, peroxidases, lipoxxygenases and other non-heme iron enzymes can catalyze this process.^{28,9c,d,e} In certain cases, lipoxxygenases, which have an iron(III) species rather than iron(IV) species serving as the key active intermediate, demonstrate even more efficient activity than P450 in *N*-dealkylation.^{9a,d} In particular, lipoxxygenases do not need an electron transfer chain to deliver electron prior to dioxygen activation.^{8a} Here, [Fe(TPA)Cl₂]Cl was employed as a catalyst for oxidative demethylation from DMA. The reactions were performed in acetonitrile with dioxygen balloon at 313 K, a list of redox inactive metal ions were scanned as Lewis acid, and the results are summarized in Table 1.

Table 1 Lewis acid triggered oxidative *N*-demethylation of *N,N*-dimethylaniline by [Fe(TPA)Cl₂]Cl catalyst with dioxygen^a

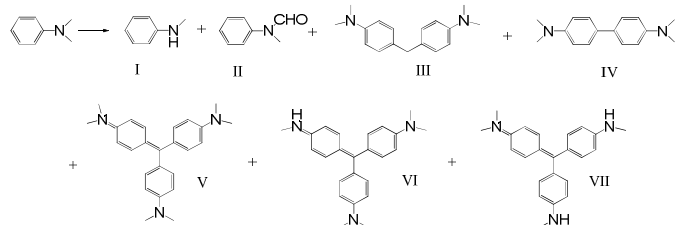
Entry	Lewis acid	Con (%)	Yield (I) (%)	Yield (II) (%)
0	-	3.5	2.0	1.2
1	NaOTf	26.9(2.1)	4.6(1.1)	2.7(0.5)
2	Zn(OTf) ₂	52.8(3.4)	5.9(1.4)	4.4(0.5)
3	Mg(OTf) ₂	27.4(3.5)	3.5(0.2)	2.7(0.3)
4	Ca(OTf) ₂	15.5(3.0)	3.4(1.4)	1.5(0.6)
5	Ba(OTf) ₂	41.1(1.7)	3.5(1.2)	3.8(0.4)
6	Al(OTf) ₃	35.1(7.0)	5.6(2.4)	2.9(1.3)
7	Sc(OTf) ₃	30.6(8.5)	3.5(0.5)	2.5(0.4)
8	Y(OTf) ₃	39.4(3.0)	6.1(1.4)	2.6(1.3)

^a Conditions: acetonitrile 5 mL, DMA 100 mM, [Fe(TPA)Cl₂]Cl 2 mM, Lewis acid 4 mM, dioxygen balloon, 313 K, 4 h. The data in parentheses represent *N*-demethylation with Lewis acid alone as catalyst in control experiments.

One may see that, in the absence of Lewis acid, [Fe(TPA)Cl₂]Cl alone is a very sluggish catalyst for *N*-demethylation reaction due to its sluggish oxidizing capability, providing only 3.5% of conversion with 2% yield of *N*-methylaniline (**I**) and 1.0% of *N*-methylformanilide (**II**) products. Adding redox inactive metal ions to [Fe(TPA)Cl₂]Cl catalyst could greatly accelerate DMA conversion, while the yields of *N*-methylaniline and *N*-methylformanilide were just slightly improved. For example, adding Al(OTf)₃ provides 35.1% of DMA conversion with 5.6% and 2.9% yields of *N*-methylaniline (**I**) and *N*-methylformanilide (**II**), respectively; adding Zn(OTf)₂ gives 52.8% conversion with 5.9% and 4.4%

yield of *N*-methylaniline and *N*-methylformanilide, respectively. As demonstrated in the parentheses of Table 1, Lewis acid alone as catalyst is inactive in control experiments. For example, in the absence of $[\text{Fe}(\text{TPA})\text{Cl}_2]\text{Cl}$, $\text{Zn}(\text{OTf})_2$ alone gave only 3.4% of conversion which is very similar with that by using $[\text{Fe}(\text{TPA})\text{Cl}_2]\text{Cl}$ alone.

Meanwhile, although adding Lewis acid can greatly accelerate the conversion of DMA, the yields of *N*-demethylation and methyl oxidation products are very low, indicating other products were generated. The detailed product isolations and identifications revealed that there exist several dimer or trimer products as shown in Scheme 1 (*N*-demethylation and methyl oxidation products were identified by GC-MS analysis (Fig. S1), and the dimer and trimer products were isolated and identified by NMR analysis (Fig. S2)). For $[\text{Fe}(\text{TPA})\text{Cl}_2]\text{Cl}/\text{Zn}(\text{OTf})_2$ mediated DMA oxidations, in addition to 5.9% yield of *N*-methylaniline and 4.4% of *N*-methylformanilide formations, it still produced 14.2% of 4,4-methylenebis(*N,N*-dimethylaniline) (**III**), 2.7% of trimer **V**, 2.7% of **VI**, with trace **IV** and **VII** formations (the yields of dimer and trimer were calculated based on DMA consumption), respectively. The formation of 4,4-methylenebis(*N,N*-dimethylaniline) (**III**) can be attributed to the reaction of DMA with formaldehyde,²⁹ where formaldehyde came from oxidative demethylation of *N,N*-dimethylaniline as reported in literatures.^{28c,e,h} Tetramethylbenzidine (**IV**) was produced by dimerization of DMA after electron transfer,³⁰ while trimers were formed by the reaction of either DMA or *N*-methylaniline with 4,4-methylenebis(*N,N*-dimethylaniline) (**III**) and their further *N*-demethylation.³¹ Similar product formations have also been observed in both lipooxygenase and chemical catalyst mediated DMA oxidations.³²



Scheme 1. Product distributions of oxidative *N*-demethylation of *N,N*-dimethylaniline by $[\text{Fe}(\text{TPA})\text{Cl}_2]\text{Cl}/\text{Zn}(\text{OTf})_2$.

Using substituted *N,N*-dimethylanilines as substrate can efficiently avoid the coupling product formation, thus improve the oxidative *N*-demethylation and methyl group oxidation product formations, and the results are summarized in Table 2. Compared with little formation of both *N*-methylaniline and *N*-methylformanilide from DMA oxidation, *p*-Me-DMA as substrate provides 31.3% yield of *p*-methyl-*N*-methylaniline with 13.7% yield of *p*-methyl-*N*-methylformanilide, and the conversion of *p*-Me-DMA is 69.6%, in which the *N*-demethylation and methyl oxidation products were identified by GC-MS analysis (Fig. S3). In the case of *p*-bromo-*N,N*-dimethylaniline (*p*-Br-DMA), it gives 16.9% yield of *p*-bromo-

N-methylaniline and 16.4% yield of *p*-bromo-*N*-methylformanilide with 54.2% of conversion. Using *p*-cyano-*N,N*-dimethylaniline (*p*-CN-DMA) as substrate just provided only 4.6% yield of *p*-cyano-*N*-methylaniline and 9.8% yield of *p*-cyano-*N*-methylformanilide with 37.7% of conversion. Interestingly, *N,N*,2,4,6-pentamethylaniline (2,4,6-Me₃PhNMe₂) as substrate only provides 27.4% yield of methyl group oxidation product (**II**), and almost no *N*-demethylation product formation. These *N*-demethylation and methyl oxidation products have been identified by NMR analysis (Fig. S4). Importantly, in the absence of $\text{Zn}(\text{OTf})_2$, $[\text{Fe}(\text{TPA})\text{Cl}_2]\text{Cl}$ is always a very sluggish catalyst for these amine oxidations as demonstrated in the parentheses of Table 2.

Table 2 Oxidative *N*-demethylation of substituted *N,N*-dimethylanilines catalyzed by $[\text{Fe}(\text{TPA})\text{Cl}_2]\text{Cl}/\text{Zn}(\text{OTf})_2$ with dioxygen.^a

Entry	Substrate	Conv. %	Yield (I) % ^b	Yield (II) % ^c
1	DMA	52.7(3.5)	5.9(1.0)	4.4(0.5)
2	<i>p</i> -Me-DMA	69.6(9.3)	31.3(6.1)	13.7(1.8)
3	<i>p</i> -Br-DMA	54.2(4.9)	16.9(0.3)	16.4(0.1)
4	<i>p</i> -CN-DMA	37.7(10.4)	4.6(0.9)	9.8(trace)
5	2,4,6-Me ₃ PhNMe ₂	49.1(0.2)	0.4(-)	27.4(-)

^a Conditions: acetonitrile 5 mL, substrate 100 mM, $[\text{Fe}(\text{TPA})\text{Cl}_2]\text{Cl}$ 2 mM, $\text{Zn}(\text{OTf})_2$ 4 mM, dioxygen balloon, 313 K, 4 h. The data in parentheses represent *N*-demethylation with $[\text{Fe}(\text{TPA})\text{Cl}_2]\text{Cl}$ alone as catalyst in control experiments. ^b The yield of substituted *N*-methylaniline product. ^c The yield of substituted *N*-methylformaniline product.

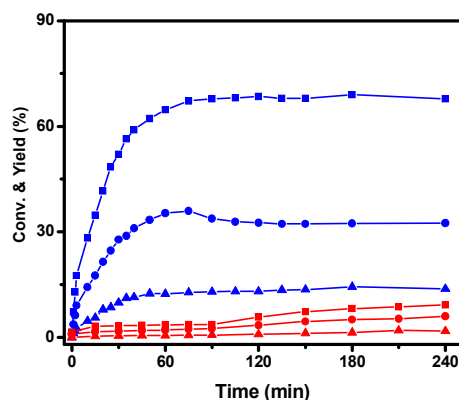


Figure 2. Catalytic kinetics for the oxidative *N*-demethylation of *p*-Me-DMA by $[\text{Fe}(\text{TPA})\text{Cl}_2]\text{Cl}$ in the presence (blue line) and absence (red line) of $\text{Zn}(\text{OTf})_2$. Conditions : acetonitrile 5 mL, *p*-Me-DMA 100 mM, $[\text{Fe}(\text{TPA})\text{Cl}_2]\text{Cl}$ 2 mM, $\text{Zn}(\text{OTf})_2$ 4 mM, dioxygen balloon, 313 K. ■ representing the conversion of *p*-Me-DMA; ● representing the yield of *p*-methyl-*N*-methylaniline; ▲ representing the yield of *p*-methyl-*N*-methylformanilide.

The promotional effect of Lewis acid was further evidenced by catalytic kinetics (Fig. 2). Clearly, adding $\text{Zn}(\text{OTf})_2$ can greatly accelerate the conversion of *p*-Me-DMA and the formations of *N*-methylation and methyl group oxidation products, while $[\text{Fe}(\text{TPA})\text{Cl}_2]\text{Cl}$ alone is very sluggish. In

addition, the influence of the ratio between $[\text{Fe}(\text{TPA})\text{Cl}_2]\text{Cl}$ and $\text{Zn}(\text{OTf})_2$ on the catalytic efficiency of DMA conversion was next investigated and displayed in Figure 3. Clearly, although Zn^{2+} is a redox inactive metal ion, adding $\text{Zn}(\text{OTf})_2$ could substantially improve the catalytic activity of $[\text{Fe}(\text{TPA})\text{Cl}_2]\text{Cl}$ complex. The sharp improvement occurs when the ratio of $\text{Zn}(\text{II})/\text{Fe}(\text{III})$ increases from 0 to 1, and it keeps improvement until the ratio goes up to 4. In Nam's work, it was observed that the interaction of Lewis acid and *N,N*-dimethylaniline would decelerate the electron transfer from DMA to the $\text{Fe}^{\text{IV}}(\text{N4Py})$ oxo species.^{30a} Here, adding $\text{Zn}(\text{OTf})_2$ to $[\text{Fe}(\text{TPA})\text{Cl}_2]\text{Cl}$ catalyst first improves its catalytic activity, then gradually retards the oxidation at high ratio of $\text{Zn}(\text{OTf})_2$ to $[\text{Fe}(\text{TPA})\text{Cl}_2]\text{Cl}$, for example, up to 6, indicating similar interaction of Zn^{2+} with DMA at high $\text{Zn}(\text{OTf})_2$ loading.

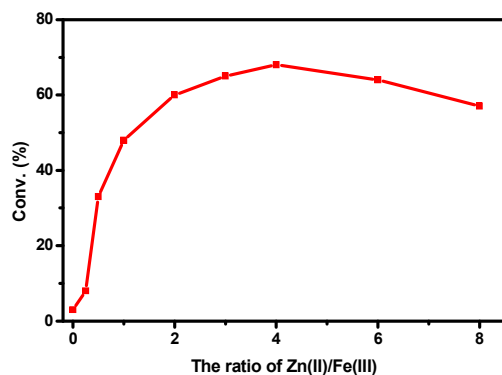


Figure 3. Influence of $\text{Zn}(\text{II})/\text{Fe}(\text{III})$ ratio on oxidative *N*-demethylation. Conditions: acetonitrile 5 mL, DMA 100 mM, $[\text{Fe}(\text{TPA})\text{Cl}_2]\text{Cl}$ 2 mM, dioxygen balloon, 313 K, 10 h.

$\text{Zn}(\text{OTf})_2$ promoted electron transfer ability of $[\text{Fe}(\text{TPA})\text{Cl}_2]\text{Cl}$ in stoichiometric reactions. In literature, it has been reported that dealkylation of amines can be initialized by electron transfer from amine to the active redox metal intermediates in both P450 enzymes and lipoygenases.^{9d,e,28d,e,32a} Here, we observed that $[\text{Fe}(\text{TPA})\text{Cl}_2]\text{Cl}$ catalyst alone is almost inactive for demethylation of DMA in a catalytic process, however, adding $\text{Zn}(\text{OTf})_2$ to the catalyst greatly promotes the oxidation of DMA. To address whether adding $\text{Zn}(\text{OTf})_2$ can improve the electron transfer capability of $[\text{Fe}(\text{TPA})\text{Cl}_2]\text{Cl}$ catalyst, stoichiometric treatments of DMA with $[\text{Fe}(\text{TPA})\text{Cl}_2]\text{Cl}$ complex in the presence and absence of $\text{Zn}(\text{OTf})_2$ were investigated through UV-Vis spectrometry, respectively. In control experiments, neither $[\text{Fe}(\text{TPA})\text{Cl}_2]\text{Cl}$ nor $\text{Zn}(\text{OTf})_2$ alone is capable of electron transfer from DMA (Fig. S5). Upon adding $\text{Zn}(\text{OTf})_2$ to the acetonitrile solution containing $[\text{Fe}(\text{TPA})\text{Cl}_2]\text{Cl}$ and DMA, it triggers an immediate electron transfer from DMA to generate tetramethylbenzidine radical cation ($\text{TMB}^{\bullet+}$) (Fig. 4a), which is similar to the oxidation of DMA by $\text{Fe}^{\text{IV}}(\text{N4Py})$ oxo in literature.^{30a} Due that the overlapping of the characteristic UV-Vis absorbance of the $\text{TMB}^{\bullet+}$ cation with $[\text{Fe}(\text{TPA})\text{Cl}_2]\text{Cl}$ happens, the disappearance

of $\text{Fe}^{\text{III}}(\text{TPA})$ species cannot be monitored by UV-Vis spectrometer. Alternatively, using *p*-Me-DMA as substrate, adding $\text{Zn}(\text{OTf})_2$ leads to immediate formation of *p*-Me-DMA radical cation ($\lambda_{\text{max}} = 465 \text{ nm}^{33}$) which further diminishes gradually. Although the decay kinetics of the $\text{Fe}^{\text{III}}(\text{TPA})$ species cannot be monitored during the rapid formation of *p*-Me-DMA radical cation, its decay and the simultaneous appearance of the corresponding $\text{Fe}^{\text{II}}(\text{TPA})$ species can be observed with the decay of the *p*-Me-DMA radical cation (Fig. 4b). In high resolution mass studies, it was also found that adding $\text{Zn}(\text{OTf})_2$ to the acetonitrile solution containing DMA and $[\text{Fe}(\text{TPA})\text{Cl}_2]\text{Cl}$ causes the immediate reduction of the $\text{Fe}^{\text{III}}(\text{TPA})$ species to the corresponding $\text{Fe}^{\text{II}}(\text{TPA})$ species, in which $[\text{Fe}(\text{TPA})\text{Cl}_2]^+$ has the mass peak at 416.0268, and it is 381.0551 for $[\text{Fe}(\text{TPA})\text{Cl}]^+$ (Fig. S6).

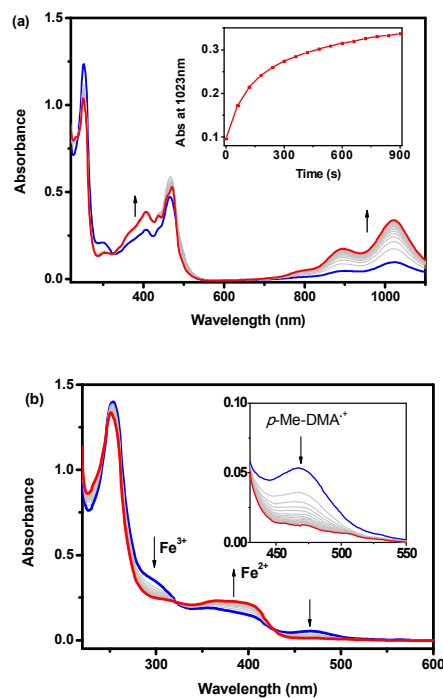


Figure 4. Kinetics of stoichiometric reactions between (a) $[\text{Fe}(\text{TPA})\text{Cl}_2]\text{Cl}$ and DMA, (b) $[\text{Fe}(\text{TPA})\text{Cl}_2]\text{Cl}$ and *p*-Me-DMA in the presence of $\text{Zn}(\text{OTf})_2$. Conditions: solvent, acetonitrile, $[\text{Fe}(\text{TPA})\text{Cl}_2]\text{Cl}$ 0.05 mM, $\text{Zn}(\text{OTf})_2$ 0.1 mM, 1 min/scan, 298 K. (a) DMA, 0.1 mM; (b) *p*-Me-DMA 0.1 mM.

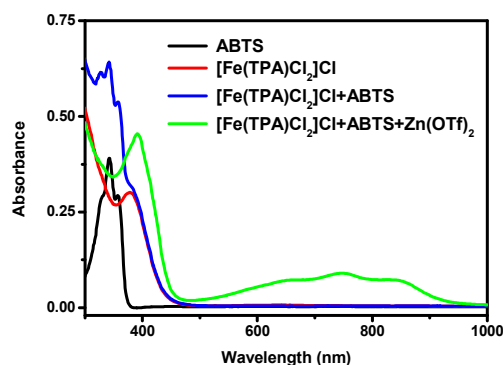


Figure 5. Zn(OTf)₂ triggered electron transfer from ABTS to [Fe(TPA)Cl₂]Cl. Conditions: solvent, acetonitrile, 298 K. ABTS (saturated) (black line); [Fe(TPA)Cl₂]Cl 0.1 mM (red line); [Fe(TPA)Cl₂]Cl 0.1 mM, ABTS (saturated) (blue line); [Fe(TPA)Cl₂]Cl 0.1 mM, ABTS (saturated), Zn(OTf)₂ 0.2 mM (green line).

2,2-Azino-di-(3-ethylbenzthiazoline-6-sulphonic acid) (ABTS) is a classical electron transfer agent to display the electron transfer ability of the active metal species.^{34,21c} ABTS itself has a characteristic absorbance at 342 nm; after the electron transfer, the generated ABTS^{•+} demonstrates its characteristic absorbance between 600 to 900 nm, which is distinctly different from that of ABTS (Fig. S7). In particular, in electron transfer from ABTS to generate ABTS^{•+}, there is no accompanied hydrogen abstract or oxygen transfer event happens, thus it is an excellent platform to disclose electron transfer without ambiguity from other oxidative events. As shown in Figure 5, adding [Fe(TPA)Cl₂]Cl to ABTS in acetonitrile does not trigger any electron transfer from ABTS to [Fe(TPA)Cl₂]Cl to generate ABTS^{•+}. However, upon adding Zn(OTf)₂ to the solution containing ABTS and [Fe(TPA)Cl₂]Cl, the absorbance of ABTS turns to that of ABTS^{•+} immediately, thus unambiguously confirms Zn(OTf)₂ enhanced electron transfer capability of the iron(III) species. Similar enhanced electron transfer capability was also verified by using ferrocene as substrate (Fig. S8).

The active iron species in the presence of Zn(OTf)₂. In literature, the iron(IV) oxo moieties have been widely investigated and proposed as the active intermediate in non-heme enzymes with their synthetic models,^{1a,b,e,35} and in DNA repair by AlkB enzyme through *N*-demethylation in which dioxygen is the terminal oxidant.³⁶ Most recently, Que, Nam and Fukuzumi proposed that Sc³⁺ can trigger or promote the formation of Fe^{IV}(TMC) oxo by dioxygen activation in the presence of BPh₄⁻ as electron donor.^{19,20} Notably, generated by oxidation of [Fe(TPA)(CH₃CN)₂]²⁺ with peracetic acid at -40°C, the Fe^{IV}(TPA) oxo moiety has been verified to be capable of transferring oxygen to cyclooctene and thioanisole.³⁷ Here, to test whether similar intermediate occurs in this Zn(OTf)₂ triggered *N*-dealkylation by [Fe(TPA)Cl₂]Cl catalyst, diphenylmethane, thioanisole and cyclooctene were independently tested as reactant to trap the potentially generated Fe^{IV}(TPA) oxo intermediate. However, with dioxygen balloon, [Fe(TPA)Cl₂]Cl does not catalyze oxidation of these substrates in the presence or absence of Zn(OTf)₂. Even in the presence of DMA, there is also no hydrogen abstraction, sulfide oxidation, or olefin epoxidation product detected in above tests. Meanwhile, there is no any characteristic UV-Vis absorbance observed for iron(IV) oxo species as reported in literatures ($\lambda_{\text{max}} \sim 724 \text{ nm}$).³⁷ Therefore, these tests clearly excluded the occurrence of the iron(IV) oxo species in present catalytic *N*-demethylation reactions. *In particular*, it has also eliminated the radical chain process happening here, otherwise, oxidations of sulfide, diphenylmethane and cyclooctene should have been observed in the presence of DMA.

On the other hand, lipoxygenases have been reported to demonstrate the co-oxidase activity in xenobiotic metabolisms

like *N*-demethylation of aminopyrine, in which electron transfer chain does not exist for dioxygen activation.^{9d,e} Although the key active intermediate for *N*-demethylation was not clearly identified, the active species in lipoxygenases is popularly proposed as an iron(III) moiety rather than iron(IV) oxo.⁸ In investigating the co-oxidase activity of lipoxygenases in demethylation of aminopyrine, Yang observed the formation of the *N*-centered aminopyrine radical, which apparently supports the initial electron transfer rather than hydrogen abstraction.^{9d} In addition, as an iron(III) intermediate in lipoxygenases, it has been convinced with synthetic models that it demonstrates a very gentle hydrogen abstraction capability.³⁸ Here, similar non-heme iron(III) species in [Fe(TPA)Cl₂]Cl is also incapable of abstracting hydrogen from diphenyl and *N*-demethylation from *N,N*-dimethylaniline, but successfully performing catalytic *N*-demethylation in the presence of Zn(OTf)₂ with dioxygen balloon, which resembles the similar dioxygenation and co-oxidase activity of lipoxygenases.^{8,9}

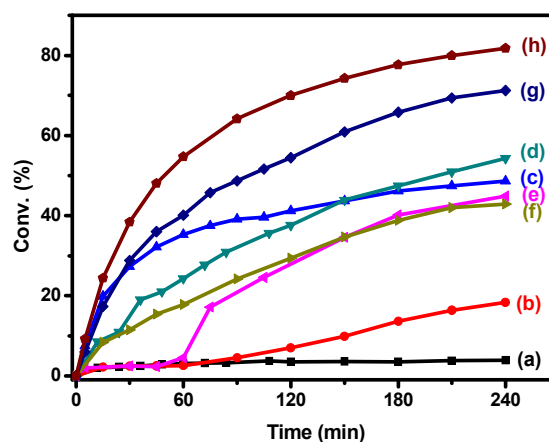


Figure 6. Catalytic oxidation kinetics of *N,N*-dimethylaniline with different catalytic systems. Conditions: acetonitrile 5 mL, DMA 100 mM, dioxygen balloon, 313 K, 4 h. (a) [Fe(TPA)Cl₂]Cl 2 mM; (b) Fe(TPA)(CH₃CN)₂(OTf)₂ 2 mM, LiCl 2 mM; (c) [Fe(TPA)Cl₂]Cl 2 mM, ZnCl₂ 4 mM; (d) [Fe(TPA)Cl₂]Cl 2 mM, Zn(OTf)₂ 4 mM; (e) Fe(TPA)Cl₂ 2 mM, Zn(OTf)₂ 4 mM; (f) Fe(TPA)(CH₃CN)₂(OTf)₂ 2 mM; (g) Fe(TPA)(CH₃CN)₂(OTf)₂ 2 mM, LiCl 2 mM, Zn(OTf)₂ 4 mM; (h) Fe(TPA)(CH₃CN)₂(OTf)₂ 2 mM, Zn(OTf)₂ 4 mM.

Next, a series of catalytic kinetics were conducted using DMA as substrate (Fig. 6). It was found that, even in the presence of Zn(OTf)₂, Fe(TPA)Cl₂ as catalyst revealed a clear induction period for DMA oxidation, whereas there is no induction period observed for [Fe(TPA)Cl₂]Cl catalyst. After the induction period, both Fe(TPA)Cl₂ and [Fe(TPA)Cl₂]Cl demonstrated a very similar kinetic behavior, suggesting that using Fe(TPA)Cl₂ as catalyst needs a relative long time to oxidize it to the active iron(III) species. However, using *p*-Me-DMA as substrate, the induction period of the Fe(TPA)Cl₂ catalyst almost disappeared (Fig. S9), indicating that the length of the induction period is substrate dependent. In high resolution mass studies, [Fe(TPA)Cl₂]Cl plus Zn(OTf)₂ in

acetonitrile revealed the mass peaks of 381.0567, 495.0389, 416.0256 and 530.0084, corresponding to $[\text{Fe}^{\text{II}}(\text{TPA})\text{Cl}]^+$, $[\text{Fe}^{\text{II}}(\text{TPA})\text{OTf}]^+$, $[\text{Fe}^{\text{III}}(\text{TPA})\text{Cl}_2]^+$, and $[\text{Fe}^{\text{III}}(\text{TPA})\text{Cl}(\text{OTf})]^+$, respectively (Fig. 7a). The occurrence of two iron(II) species can be attributed to the *in situ* reduction of the corresponding iron(III) species under mass analytic conditions. For the $\text{Fe}(\text{TPA})\text{Cl}_2$ plus $\text{Zn}(\text{OTf})_2$, it revealed the mass peaks of 381.0566 and 495.0407, corresponding to $[\text{Fe}^{\text{II}}(\text{TPA})\text{Cl}]^+$ and $[\text{Fe}^{\text{II}}(\text{TPA})\text{OTf}]^+$ species, while the $[\text{Fe}^{\text{II}}(\text{TPA})\text{OTf}]^+$ species are dominant (Fig. 7b). Consistent with this, adding $\text{Zn}(\text{OTf})_2$ to the acetonitrile solution of $\text{Fe}(\text{TPA})\text{Cl}_2$ changes its UV-Vis spectrum a lot, clearly indicating the formation of $\text{Fe}(\text{TPA})(\text{OTf})_2$ as those in literature (Fig. 8).^{27,39} Although adding $\text{Zn}(\text{OTf})_2$ to the acetonitrile solution of $[\text{Fe}(\text{TPA})\text{Cl}_2]\text{Cl}$ does not show so remarkable UV-Vis spectrum change as that of $\text{Fe}(\text{TPA})\text{Cl}_2$, it also shifts its characteristic absorbance slightly. $[\text{Fe}(\text{TPA})\text{Cl}_2]\text{Cl}$ alone in acetonitrile revealed a characteristic band having maximum absorbance at 380 nm; upon adding $\text{Zn}(\text{OTf})_2$, the characteristic absorbance of the iron(III) species slightly decreases with minor but nonetheless blue shift, and specially, it demonstrates two clear isosbestic points around 314 and 363 nm (Fig. S10). Changing the ratio of $\text{Zn}(\text{OTf})_2$ and $[\text{Fe}(\text{TPA})\text{Cl}_2]\text{Cl}$ further evidenced the blue shift of this absorbance band, indicating the formation of new iron(III) species (Fig. 9a).

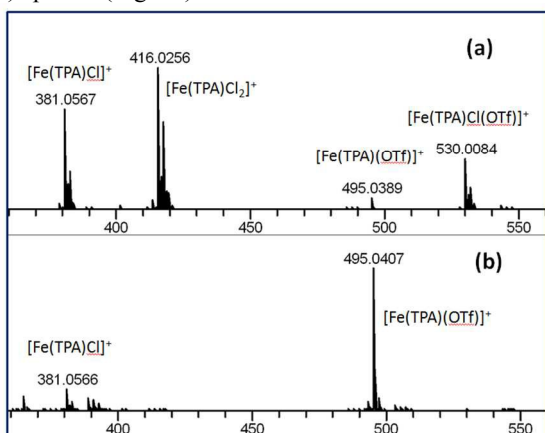


Figure 7. Mass spectra of (a) $[\text{Fe}(\text{TPA})\text{Cl}_2]\text{Cl}$ 2 mM, $\text{Zn}(\text{OTf})_2$ 4 mM; (b) $\text{Fe}(\text{TPA})\text{Cl}_2$ 2 mM, $\text{Zn}(\text{OTf})_2$ 4 mM in acetonitrile.

One may argue that the UV-Vis absorbance change by adding $\text{Zn}(\text{OTf})_2$ to $[\text{Fe}(\text{TPA})\text{Cl}_2]\text{Cl}$ is due to the minor formation of OTf^- anion ligated iron(III) species as disclosed in its mass spectra. However, similar blue shifts have been observed by adding $\text{Al}(\text{OTf})_3$, $\text{Sc}(\text{OTf})_3$, $\text{Mg}(\text{OTf})_2$, $\text{Ca}(\text{OTf})_2$ and even ZnCl_2 to the acetonitrile solution of $[\text{Fe}(\text{TPA})\text{Cl}_2]\text{Cl}$ complex (Fig. S11). In particular, adding $\text{Al}(\text{OTf})_3$ shifts the absorbance of the iron(III) species significantly from 380 to 364 nm, and changing the ratio of $\text{Al}(\text{OTf})_3$ and $[\text{Fe}(\text{TPA})\text{Cl}_2]\text{Cl}$ much more clearly displays the blue shift of the iron(III) species with three isosbestic points around 279, 298 and 384 nm (Fig. 9b). More importantly, in high resolution mass spectrum, adding $\text{Al}(\text{OTf})_3$ to the acetonitrile solution of $[\text{Fe}(\text{TPA})\text{Cl}_2]\text{Cl}$ revealed that

there are only mass peaks of 381.0569 and 416.0257, corresponding to $[\text{Fe}^{\text{II}}(\text{TPA})\text{Cl}]^+$ and $[\text{Fe}^{\text{III}}(\text{TPA})\text{Cl}_2]^+$, without OTf^- ligated iron(III) species formation (Fig. 10a), thus eliminated the disturbing from the formation of OTf^- ligated iron(III) species in its UV-Vis spectrum. Moreover, adding ZnCl_2 also revealed a slight blue-shift as well as adding $\text{Zn}(\text{OTf})_2$ (Fig. S11), which clearly excluded the possibility of the blue-shift originating from formation of minor OTf^- ligated iron(III) species like $[\text{Fe}(\text{TPA})\text{Cl}(\text{OTf})]^+$. In addition, catalytic kinetics revealed that both adding $\text{Al}(\text{OTf})_3$ and ZnCl_2 generate similar promotional effect in oxidative dealkylation of DMA as well as adding $\text{Zn}(\text{OTf})_2$ (Fig. S12).

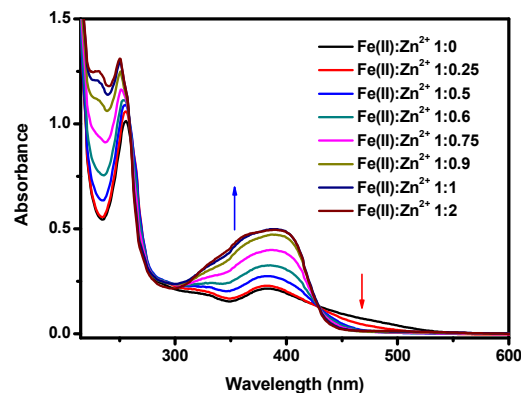


Figure 8. UV-Vis spectra of $\text{Fe}(\text{TPA})\text{Cl}_2$ with $\text{Zn}(\text{OTf})_2$ in acetonitrile under different Fe(II)/Zn(II) ratio. Conditions: solvent, acetonitrile, 298 K. $\text{Fe}(\text{TPA})\text{Cl}_2$ 0.1 mM (black line); $\text{Fe}(\text{TPA})\text{Cl}_2$ 0.1 mM, $\text{Zn}(\text{OTf})_2$ 0-0.2 mM.

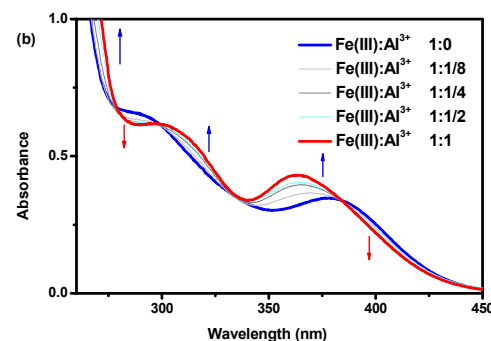
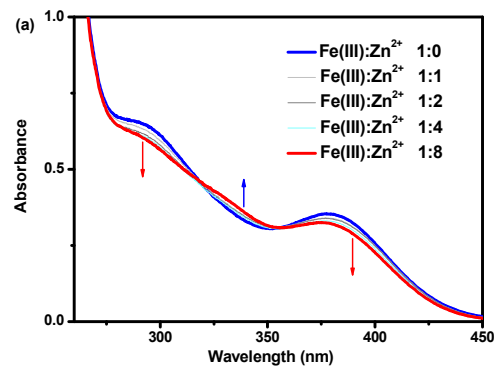


Figure 9. UV-Vis absorbance change by adding different amounts of $\text{Zn}(\text{OTf})_2$ or $\text{Al}(\text{OTf})_3$ to $[\text{Fe}(\text{TPA})\text{Cl}_2]\text{Cl}$. Conditions: solvent, acetonitrile, 298 K. (a) $[\text{Fe}(\text{TPA})\text{Cl}_2]\text{Cl}$ 0.1 mM, $\text{Zn}(\text{OTf})_2$ 0-0.8 mM; (b) $[\text{Fe}(\text{TPA})\text{Cl}_2]\text{Cl}$ 0.1 mM, $\text{Al}(\text{OTf})_3$ 0-0.1 mM.

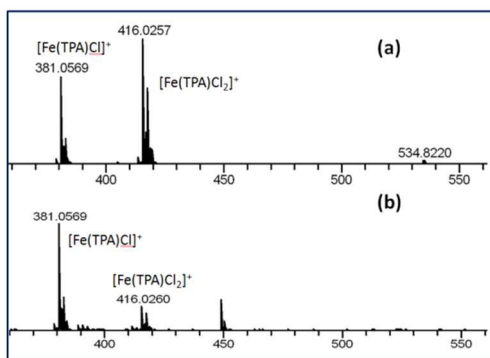


Figure 10. Mass spectra of (a) $[\text{Fe}(\text{TPA})\text{Cl}_2]\text{Cl}$ 2 mM, $\text{Al}(\text{OTf})_3$ 4 mM; (b) $[\text{Fe}(\text{TPA})\text{Cl}_2]\text{Cl}$ 2 mM, ZnCl_2 4 mM in acetonitrile.

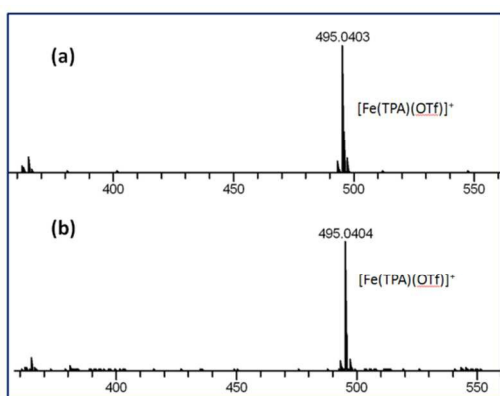


Figure 11. Mass spectra of (a) $\text{Fe}(\text{TPA})(\text{CH}_3\text{CN})_2(\text{OTf})_2$ 2 mM; (b) $\text{Fe}(\text{TPA})(\text{CH}_3\text{CN})_2(\text{OTf})_2$ 2mM, $\text{Zn}(\text{OTf})_2$ 4 mM in acetonitrile.

Notably, unlike sluggish $[\text{Fe}(\text{TPA})\text{Cl}_2]\text{Cl}$, using $\text{Fe}(\text{TPA})(\text{CH}_3\text{CN})_2(\text{OTf})_2$ alone as catalyst demonstrated a remarkable activity in catalytic DMA oxidation, even though it is still less active than $[\text{Fe}(\text{TPA})\text{Cl}_2]\text{Cl}/\text{Zn}(\text{OTf})_2$ (Fig. 6, see above). In particular, adding $\text{Zn}(\text{OTf})_2$ to $\text{Fe}(\text{TPA})(\text{CH}_3\text{CN})_2(\text{OTf})_2$ further promotes its catalytic activity greatly. In high resolution mass studies, both $\text{Fe}(\text{TPA})(\text{CH}_3\text{CN})_2(\text{OTf})_2$ and $\text{Fe}(\text{TPA})(\text{CH}_3\text{CN})_2(\text{OTf})_2/\text{Zn}(\text{OTf})_2$ systems revealed similar iron species, that is, only $[\text{Fe}(\text{TPA})(\text{OTf})]^+$ (495.0403 vs 495.0404) was clearly observed (Fig. 11), while their UV-Vis spectra are also very similar (Fig. S13). Since there is no chloride in the reaction solution of the $\text{Fe}(\text{TPA})(\text{CH}_3\text{CN})_2(\text{OTf})_2/\text{Zn}(\text{OTf})_2$ system, and the counterion for both Fe^{3+} and Zn^{2+} cations is OTf^- , the promotional effect by adding $\text{Zn}(\text{OTf})_2$ should be unambiguously attributed to the Zn^{2+} rather than OTf^- anion, which is similar with that of adding ZnCl_2 to $[\text{Fe}(\text{TPA})\text{Cl}_2]\text{Cl}$. In another kinetic experiment, adding LiCl to $\text{Fe}(\text{TPA})(\text{CH}_3\text{CN})_2(\text{OTf})_2$ greatly reduces its catalytic activity, even slower than all of tests having $\text{Zn}(\text{OTf})_2$

added, and its high resolution mass spectrum revealed the formation of dominant $[\text{Fe}(\text{TPA})\text{Cl}]^+$ species (381.0562) with minor $[\text{Fe}(\text{TPA})(\text{OTf})]^+$ species (495.0399) (Fig. S14a). Significantly, adding $\text{Zn}(\text{OTf})_2$ to above $\text{Fe}(\text{TPA})(\text{CH}_3\text{CN})_2(\text{OTf})_2/\text{LiCl}$ system recovers its catalytic activity, and the high resolution mass still revealed the existence of $[\text{Fe}(\text{TPA})\text{Cl}]^+$ species (381.0550), but dominates with $[\text{Fe}(\text{TPA})(\text{OTf})]^+$ species (495.0400) (Fig. S14b). Moreover, adding ZnCl_2 to the $[\text{Fe}(\text{TPA})\text{Cl}_2]\text{Cl}$ catalyst generates similar catalytic kinetics with that of adding $\text{Zn}(\text{OTf})_2$. Notably, the high resolution mass of $[\text{Fe}(\text{TPA})\text{Cl}_2]\text{Cl}/\text{ZnCl}_2$ revealed that most of $[\text{Fe}(\text{TPA})\text{Cl}_2]\text{Cl}$ complex has been reduced to the iron(II) species having mass peak of $[\text{Fe}(\text{TPA})\text{Cl}]^+$ species (381.0569), also implicating the improved redox possibility of the iron(III) species in the presence of ZnCl_2 under mass analytic conditions (Fig. 10b). Taken together, the catalytic activity series of the $\text{Fe}^{\text{III}}(\text{TPA})$ species in DMA oxidation can be summarized as follows:

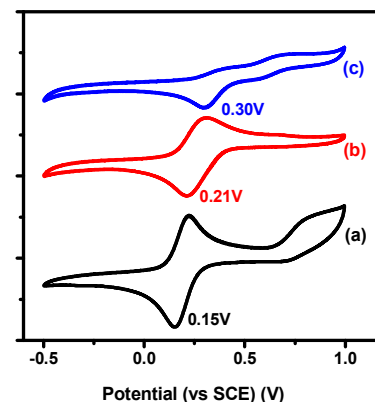
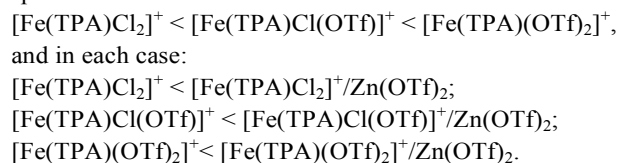


Figure 12. Cyclic voltammograms of $[\text{Fe}(\text{TPA})\text{Cl}_2]\text{Cl}$ in the presence/absence of Zn^{2+} . Conditions: solvent, dry acetonitrile, tetrabutylammonium perchlorate 0.1 M, 50 mV/s, 298 K, under nitrogen. (a) $[\text{Fe}(\text{TPA})\text{Cl}_2]\text{Cl}$ 2 mM (black line); (b) $[\text{Fe}(\text{TPA})\text{Cl}_2]\text{Cl}$ 2 mM, ZnCl_2 4 mM (red line); (c) $[\text{Fe}(\text{TPA})\text{Cl}_2]\text{Cl}$ 2 mM, $\text{Zn}(\text{OTf})_2$ 4 mM (blue line).

Improved electron transfer ability of the iron(III) species by adding Zn^{2+} was further evidenced by electrochemical studies. As shown in Figure 12, adding ZnCl_2 to $[\text{Fe}(\text{TPA})\text{Cl}_2]\text{Cl}$ in acetonitrile positively shifts the redox potential of the $\text{Fe}^{\text{II}}/\text{Fe}^{\text{III}}$ couple from +0.15 V to +0.21 V (vs SCE), while adding $\text{Zn}(\text{OTf})_2$ slightly more shifts the potential to +0.30 V (vs SCE). Similar positively shifting of potentials have been observed by adding redox inactive metals to manganese(IV) complexes in previous studies.^{18,23a} In addition, the EPR studies provided the complimentary clues of their interaction (Fig. 13). In dry acetonitrile at 130 K, the EPR spectrum of the $[\text{Fe}(\text{TPA})\text{Cl}_2]\text{Cl}$

complex reveals that it is typical of high-spin state having g value of 4.167.⁴⁰ The same high spin state was also found in lipoyxygenases and some synthetic models.^{8f,41} Upon adding $\text{Zn}(\text{OTf})_2$, although it does not change its spin state, it still clearly affects the EPR signal of the $[\text{Fe}(\text{TPA})\text{Cl}_2]\text{Cl}$, and reveals a g value of 4.194. Similar influences on EPR signal have also been observed by adding $\text{Sc}(\text{OTf})_3$, $\text{Al}(\text{OTf})_3$ and $\text{Mg}(\text{OTf})_2$, giving g values of 4.195, 4.159 and 4.192, respectively. Taken together, it has apparently suggested that there exists the interaction between the $\text{Fe}^{\text{III}}(\text{TPA})$ species and added Lewis acid through plausible chloride or OTf bridge, which has blue-shifted the UV-Vis absorbance, positively shifted the redox potential, changed the EPR signal, and improved the electron transfer capability of the $\text{Fe}^{\text{III}}(\text{TPA})$ species in amine oxidation. Certainly, the extra Zn^{2+} cation may also serve pulling chloride anion from $[\text{Fe}(\text{TPA})\text{Cl}_2]\text{Cl}$ catalyst, since formation of $[\text{Fe}^{\text{III}}(\text{TPA})(\text{Cl})(\text{OTf})]^+$ has been indicated by adding $\text{Zn}(\text{OTf})_2$ to the acetonitrile solution of $[\text{Fe}(\text{TPA})\text{Cl}_2]\text{Cl}$ complex (see Fig.7a above). The missing of binding information of Zn^{2+} with $\text{Fe}^{\text{III}}(\text{TPA})$ complex in mass studies can be attributed to its fragility and easily broken under the mass conditions. Similar blue-shift of the manganese(IV) complexes by adding Lewis acids was also observed in previous studies which revealed the interaction of the Lewis acid with the manganese(IV) complex.^{18,23a}

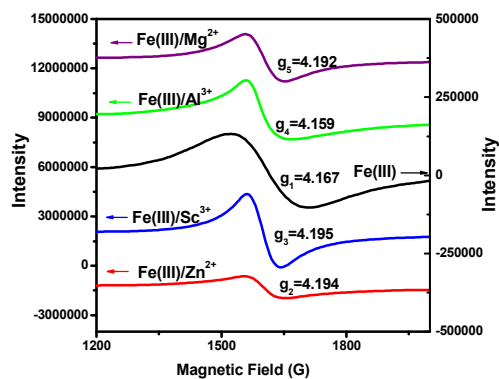


Figure 13. EPR spectra of $[\text{Fe}(\text{TPA})\text{Cl}_2]\text{Cl}$ in the presence of different Lewis acids. Conditions: solvent, acetonitrile, 130 K. $[\text{Fe}(\text{TPA})\text{Cl}_2]\text{Cl}$ 5 mM (black line); $[\text{Fe}(\text{TPA})\text{Cl}_2]\text{Cl}$ 5 mM, $\text{Zn}(\text{OTf})_2$ 10 mM (red line); $[\text{Fe}(\text{TPA})\text{Cl}_2]\text{Cl}$ 5 mM, $\text{Sc}(\text{OTf})_3$ 10 mM (blue line); $[\text{Fe}(\text{TPA})\text{Cl}_2]\text{Cl}$ 5 mM, $\text{Al}(\text{OTf})_3$ 10 mM (green line); $[\text{Fe}(\text{TPA})\text{Cl}_2]\text{Cl}$ 5 mM, $\text{Mg}(\text{OTf})_2$ 10 mM (purple line).

Mechanism of Lewis acid promoted demethylation of amine with $[\text{Fe}(\text{TPA})\text{Cl}_2]\text{Cl}/\text{Zn}(\text{OTf})_2$. In literature, both electron transfer (ET) and hydrogen abstraction mechanisms have been proposed for N -dealkylation by P450 enzymes, peroxidases, lipoyxygenases and their models.^{9,28,32a,42} In DMA, the bond dissociation energy of the C-H bond (BDE_{CH}) in methyl group is about 92 kcal/mol.⁴³ In this study, diphenylmethane, which has a BDE_{CH} value of 82 kcal/mol, has been employed as substrate to test the hydrogen abstraction ability of $[\text{Fe}(\text{TPA})\text{Cl}_2]\text{Cl}/\text{Zn}(\text{OTf})_2$, however, there was no hydrogen abstraction reaction observed (*vide supra*). Even using 1,4-

cyclohexadiene as substrate having a BDE_{CH} value of 76 kcal/mol, it has only trace hydrogen abstraction product benzene formed, supporting that the oxidative N -demethylation demonstrated here does not proceed by hydrogen abstraction at the initial step. Furthermore, as stated above, $[\text{Fe}(\text{TPA})\text{Cl}_2]\text{Cl}/\text{Zn}(\text{OTf})_2$ has demonstrated its capability in electron transfer from both DMA and ABTS in stoichiometric oxidations (see Fig. 4a and 5), and electrochemical studies also disclosed its positive shift of redox potential by adding $\text{Zn}(\text{II})$ salts (see Fig. 12). Clearly, this $[\text{Fe}(\text{TPA})\text{Cl}_2]\text{Cl}/\text{Zn}(\text{OTf})_2$ mediated oxidative demethylation is initialized by electron transfer rather than hydrogen abstraction. In addition, no saturation kinetics was observed in oxidative N -demethylation of p -Me-DMA in the substrate concentration range of 50-800 mM (Fig. 14), suggesting that the formation of the pre-complex between substrate and catalyst does not occur prior to electron transfer, thus implicates that it is an outer-sphere electron transfer process.

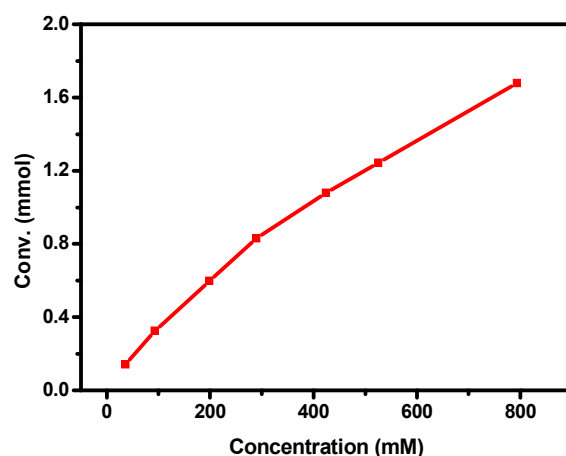


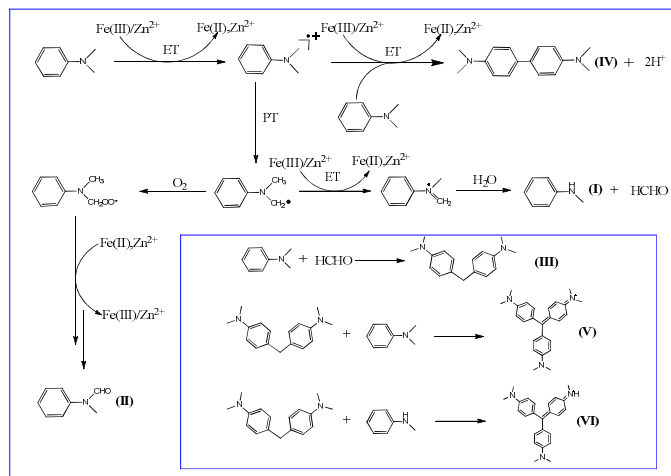
Figure 14. Saturation behavior of $[\text{Fe}(\text{TPA})\text{Cl}_2]\text{Cl}/\text{Zn}(\text{OTf})_2$ mediated oxidative dealkylation. Conditions: acetonitrile 5 mL, p -Me-DMA (50-800 mM), $[\text{Fe}(\text{TPA})\text{Cl}_2]\text{Cl}$ 2 mM, $\text{Zn}(\text{OTf})_2$ 4 mM, dioxygen balloon, 313 K, 4 h.

As disclosed earlier, using $\text{Fe}(\text{TPA})\text{Cl}_2$ as the iron source would cause a long induction period, indicating that oxidizing of the dication iron(II) to the active trication iron(III) species by dioxygen is very slow, even in the presence of Zn^{2+} . The sluggish oxidation of $\text{Fe}^{\text{II}}(\text{TPA})$ to $\text{Fe}^{\text{III}}(\text{TPA})$ species has also been evidenced by UV-Vis studies in which the UV-Vis absorbance changes very slowly (Fig. S15). After the induction period, $\text{Fe}(\text{TPA})\text{Cl}_2$ and $[\text{Fe}(\text{TPA})\text{Cl}_2]\text{Cl}$ demonstrated an identical kinetic behavior for DMA oxidation, apparently suggesting that regenerating of the active iron(III) species may not proceed by oxidizing of the reduced iron(II) species with dioxygen directly, but by the oxidative intermediate generated in DMA oxidation, which resembles the dioxygenation and co-oxidase activity of lipoyxygenases.^{8,9} In addition, the length of induction period is substrate dependent (*vide supra*), which further supports this conclusion. The oxidation of DMA is a

complicated reaction as there are a list of product formations along with the formation of *N*-methylaniline and *N*-methylformaniline (see Scheme 1 above). Similar complicated product distributions have also been reported in lipoxygenases mediated *N*-demethylation, electrochemical oxidation of DMA and other studies.^{31,32} However, a radical chain process may not happen here, since using diphenylmethane, sulfide or cyclooctene as substrate did not generate any observed hydrogen abstraction or oxygenation product, even in the presence of DMA (*vide supra*). Taken together, a simplified mechanism for [Fe(TPA)Cl₂]Cl/Zn(OTf)₂ mediated oxidative demethylation of DMA has been proposed as Scheme 2.

First, in the presence of Zn²⁺, the oxidation was triggered by electron transfer from DMA to Fe^{III}(TPA) species to generate the DMA^{•+} with reduced Fe^{II}(TPA) species formation. DMA^{•+} may undergo dimerization via the reaction with another DMA to produce tetramethylbenzidine (TMB). In stoichiometric oxidation monitored by UV-Vis, TMB can be further oxidized to TMB^{•+} having characteristic absorption at 470, 900, and 1023 nm, while the characteristic absorbance of DMA^{•+} was also observed at 465 nm (Fig. 4a).⁴⁴ More importantly, the generated DMA^{•+} can also undergo proton transfer to produce DMA[•] free radical, then the DMA[•] radical can be trapped by dioxygen to generate a peroxy radical intermediate which next oxidizes the reduced Fe^{II}(TPA) species back to the active Fe^{III}(TPA) species with the formation of *N*-methylformanilide product, which is the key step to achieve the catalytic cycle of the iron species. In lipoxygenases, similar regeneration of the active iron(III) species by oxidation of reduced iron(II) species with unsaturated fatty acid peroxy radical, generated by dioxygen trapping of substrate radical, has also been proposed to achieve the catalytic cycle.^{8a} On the other hand, DMA[•] radical can also transfer electron to another Fe^{III}(TPA) species to form an iminium cation which next undergoes hydrolysis to generate *N*-methylaniline and formaldehyde. The generated formaldehyde next reacts with DMA to produce 4,4-methylenebis(*N,N*-dimethylaniline) (III) which can further proceed electron transfer and polymerization to form trimers as shown in Scheme 1. Similar dimer and trimer formations have been reported elsewhere.^{31,32}

Clearly, in this Zn²⁺ triggered amine oxidations with [Fe(TPA)Cl₂]Cl catalyst, the external electron donor is not essential for dioxygen activation as well as that in lipoxygenases. In nature, lipoxygenases can carry out efficient electron transfer from amines to its iron(III) intermediate in its co-oxidase activity of xenobiotic metabolisms,⁹ however, in a chemical process, the iron(III) species in [Fe(TPA)Cl₂]Cl is very sluggish to achieve this event. Alternatively, inspired by non-redox metal ions promoted stoichiometric and catalytic oxidations by redox metal oxo moieties,^{12-15,23a} herein, binding non-redox metal ions like Zn²⁺ to the iron(III) species also improves the oxidizing power of Fe^{III}(TPA) complex, which triggers the electron transfer from DMA to the iron(III) species, and initializes the efficient catalytic cycle with dioxygen activation.



Scheme 2. Simplified mechanism for *N,N*-dimethylaniline oxidation.

Conclusions

Inspired by the dioxygenation and co-oxidase activity of lipoxygenases, this work illustrated an alternative protocol to activate dioxygen in a catalytic process at ambient temperature without utilizing external electron donors. That is, through binding redox inactive metal ions, the oxidizing power of these normally stable redox metal ions can be promoted to be able to oxidize substrate, thus initialize the catalytic cycle with dioxygen activation as well as lipoxygenases. In oxidation of *N,N*-dimethylaniline and its analogues with dioxygen, using [Fe(TPA)Cl₂]Cl alone as catalyst is very sluggish, whereas adding redox inactive metal ions like Zn²⁺ greatly improve the oxidizing power of the iron(III) species, thus trigger the catalytic cycle with dioxygen activation. It was further found that oxidation of amines is initialized by electron transfer rather than hydrogen abstraction, and the iron(IV) species does not occur in reaction solution. The improved electron transfer capability of iron(III) species was evidenced by stoichiometric oxidation of amines and ATBS. Detailed reaction kinetics with UV-Vis, high resolution mass, electrochemistry and EPR studies indicated that there exists interaction between added Zn²⁺ with Fe^{III}(TPA) species plausible through chloride or OTf anion, which improves its oxidizing power to initialize the catalytic oxidation with dioxygen. This work demonstrated a new strategy to activate these sluggish redox catalysts to utilize dioxygen in a catalytic process at ambient temperature where the external electron donor is not essential.

Under the review of this work, it was reported that the Sc³⁺ bound iron(IV) oxo X-ray crystal structure¹⁶ is actually a Sc³⁺-O-Fe³⁺ species.⁴⁵ This new findings may also implicate that the interaction of Sc³⁺ with iron(IV) oxo leads to the reduction of the iron(IV) oxo through electron transfer to form the identified Sc³⁺-O-Fe³⁺ species.

ACKNOWLEDGMENT This work was supported by the National Natural Science Foundation of China (No 21273086 and 21303063). The GC-MS and NMR analysis were

performed in the Analytical and Testing Center of Huazhong University of Science and Technology.

Notes and references

School of Chemistry and Chemical Engineering, Huazhong University of Science and Technology. Key Laboratory for Large-Format Battery Materials and System, Ministry of Education. Luoyu Road 1037, Wuhan 430074, PR China. E-mail: gyin@hust.edu.cn.

Electronic Supplementary Information (ESI) available: GC-MS and NMR data of oxidation products, UV-Vis spectra and high resolution mass of iron species under different conditions, oxidation kinetics of DMA by [Fe(TPA)Cl₂]Cl catalyst in the presence of Al(OTf)₃. See DOI: 10.1039/c000000x/

- (a) W. Nam, *Acc. Chem. Res.* **2007**, *40*, 522; (b) L. Que Jr. *Acc. Chem. Res.* **2007**, *40*, 493; (c) J. M. Mayer, *Acc. Chem. Res.* **2011**, *44*, 36; (d) A. S. Borovik, *Acc. Chem. Res.* **2005**, *38*, 54; (e) W. Nam, Y. M. Lee and S. Fukuzumi, *Acc. Chem. Res.* **2014**, *47*, 1146; (f) W. L. Man, W. W. Y. Lam and T. C. Lau, *Acc. Chem. Res.* **2014**, *47*, 427; (g) D. P. Goldberg, *Acc. Chem. Res.* **2007**, *40*, 626; (h) R. A. Geiger, S. Chattopadhyay, V. W. Day and T. A. Jackson, *J. Am. Chem. Soc.* **2010**, *132*, 2821; (i) S. Chattopadhyay, R. A. Geiger, G. Yin, D. H. Busch and T. A. Jackson, *Inorg. Chem.* **2010**, *49*, 7530.
- (a) J. A. Kovacs, *Science* **2003**, *299*, 1024; (b) C. E. MacBeth, A. P. Golombok, V. G. Young Jr., C. Yang, K. Kuczera, M. P. Hendrich and A. S. Borovik, *Science* **2000**, *289*, 938; (c) M. Costas, M. P. Mehn, M. P. Jensen and L. Que Jr. *Chem. Rev.* **2004**, *104*, 939; (d) H. Chen, K. B. Cho, W. Lai, W. Nam and S. Shaik, *J. Chem. Theory Comput.* **2012**, *8*, 915; (e) S. Hong, Y. M. Lee, W. Shin, S. Fukuzumi and W. Nam, *J. Am. Chem. Soc.* **2009**, *131*, 13910; (f) A. Thibon, J. England, M. Martinho, V. G. Young Jr., J. R. Frisch, R. Guillot, J. J. Girerd, E. Münck, L. Que Jr. and F. Banse, *Angew. Chem., Int. Ed.* **2008**, *47*, 7064; (g) Y. J. Sun, Q. Q. Huang, T. Tano and S. Itoh, *Inorg. Chem.* **2013**, *52*, 10936.
- A. Ghosh, F. T. de Oliveira, T. Yano, T. Nishioka, E. S. Beach, I. Kinoshita, E. Münck, A. D. Ryabov, C. P. Horwitz and T. J. Collins, *J. Am. Chem. Soc.* **2005**, *127*, 2505.
- (a) A. Company, L. Gómez, M. Güell, X. Ribas, J. M. Luis, L. Que Jr. and M. Costas, *J. Am. Chem. Soc.* **2007**, *129*, 15766; (b) A. Ghosh, D. A. Mitchell, A. Chanda, A. D. Ryabov, D. L. Popescu, E. C. Upham, G. J. Collins and T. J. Collins, *J. Am. Chem. Soc.* **2008**, *130*, 15116; (c) B. Wang, S. Wang, C. Xia and W. Sun, *Chem.-Eur. J.* **2012**, *18*, 7332; (d) M. N. Bhakta, P. F. Hollenberg and K. Wimalasena, *J. Am. Chem. Soc.* **2005**, *127*, 1376; (e) A. Murphy, G. Dubois and T. D. P. Stack, *J. Am. Chem. Soc.* **2003**, *125*, 5250.
- (a) A. Mahammed, H. B. Gray, A. E. Meier-Callahan and Z. Gross, *J. Am. Chem. Soc.* **2003**, *125*, 1162; (b) J. Rosenthal, B. J. Pistorio, L. L. Chng and D. G. Nocera, *J. Org. Chem.* **2005**, *70*, 1885; (c) A. E. Wendlandt and S. S. Stahl, *J. Am. Chem. Soc.* **2014**, *136*, 506; (d) A. Sobkowiak and D. T. Sawyer, *J. Am. Chem. Soc.* **1991**, *113*, 9520; (e) S. Itoh, H. Kumei, M. Taki, S. Nagatomo, T. Kitagawa and S. Fukuzumi, *J. Am. Chem. Soc.* **2001**, *123*, 6708.
- (a) B. Meunier, S. P. de Visser and S. Shaik, *Chem. Rev.* **2004**, *104*, 3947; (b) G. Yin, *Coord. Chem. Rev.* **2010**, *254*, 1826; (c) I. G. Denisov, T. M. Makris, S. G. Sligar and I. Schlichting, *Chem. Rev.* **2005**, *105*, 2253; (d) M. Sono, M. P. Roach, E. D. Coulter and J. H. Dawson, *Chem. Rev.* **1996**, *96*, 2841; (e) F. P. Guengerich and T. L. Macdonald, *Acc. Chem. Res.* **1984**, *17*, 9.
- (a) L. Que Jr. and Y. Dong, *Acc. Chem. Res.* **1996**, *29*, 190; (b) M. H. Baik, M. Newcomb, R. A. Friesner and S. J. Lippard, *Chem. Rev.* **2003**, *103*, 2385; (c) L. J. Murray and S. J. Lippard, *Acc. Chem. Res.* **2007**, *40*, 466; (d) C. E. Tinberg and S. J. Lippard, *Acc. Chem. Res.* **2011**, *44*, 280.
- (a) J. P. Klinman, *Acc. Chem. Res.* **2007**, *40*, 325; (b) S. T. Prigge, J. C. Boyington, M. Faig, K. S. Doctor, B. J. Gaffney and L. M. Amzel, *Biochimie* **1997**, *79*, 629; (c) M. L. Neidig, A. T. Weckler, G. Schenk, T. R. Holman and E. I. Solomon, *J. Am. Chem. Soc.* **2007**, *129*, 7531; (d) N. Lehnert and E. I. Solomon, *J. Biol. Inorg. Chem.* **2003**, *8*, 294; (e) M. H. Glickman and J. P. Klinman, *Biochem.* **1996**, *35*, 12882; (f) E. I. Solomon, T. C. Brunold, M. I. Davis, J. N. Kemsley, S. K. Lee, N. Lehnert, F. Neese, A. J. Skulan, Y. S. Yang and J. Zhou, *Chem. Rev.* **2000**, *100*, 235; (g) M. M. Abu-Omar, A. Loaiza and N. Hontzeas, *Chem. Rev.* **2005**, *105*, 2227.
- (a) A. P. Kulkarni, *Cell. Mol. Life. Sci.* **2001**, *58*, 1805; (b) J. Hu and A. P. Kulkarni, *Teratog. Carcinog. Mutagen.* **2000**, *20*, 195; (c) J. Hu and A. P. Kulkarni, *Pestic. Biochem. Phys.* **1998**, *61*, 145; (d) X. Yang and A. P. Kulkarni, *J. Biochem. Mol. Toxic.* **1998**, *12*, 175; (e) M. Pérez-Gilbert, A. Sánchez-Ferrer and F. Garcia-Carmona, *Free. Radical. Bio. Med.* **1997**, *23*, 548.
- (a) W. Kuang, Y. Fan, J. Qiu and Y. Chen, *J. Mater. Chem.* **1998**, *8*, 19; (b) G. Gündüz and O. Akpolat, *Ind. Eng. Chem. Res.* **1990**, *29*, 45.
- (a) E. M. Sproviero, J. A. Gascón, J. P. McEvoy, G. W. Brudvig and V. S. Batista, *J. Am. Chem. Soc.* **2008**, *130*, 3428; (b) J. P. McEvoy and G. W. Brudvig, *Chem. Rev.* **2006**, *106*, 4455.
- (a) T. C. Lau, Z. B. Wu, Z. L. Bai and C. K. Mak, *J. Chem. Soc., Dalton Trans.* **1995**, *4*, 695; (b) W. W. Y. Lam, S. M. Yiu, J. M. N. Lee, S. K. Y. Yau, H. K. Kwong, T. C. Lau, D. Liu and Z. Lin, *J. Am. Chem. Soc.* **2006**, *128*, 2851.
- C. G. Miller, S. W. Gordon-Wylie, C. P. Horwitz, S. A. Strazisar, D. K. Peraino, G. R. Clark, S. T. Weintraub and T. J. Collins, *J. Am. Chem. Soc.* **1998**, *120*, 11540.
- (a) J. Park, Y. Morimoto, Y. M. Lee, W. Nam and S. Fukuzumi, *J. Am. Chem. Soc.* **2011**, *133*, 5236; (b) J. Chen, Y. M. Lee, K. M. Davis, X. Wu, M. S. Seo, K. B. Cho, H. Yoon, Y. J. Park, S. Fukuzumi, Y. N. Pushkar and W. Nam, *J. Am. Chem. Soc.* **2013**, *135*, 6388; (c) J. Park, Y. Morimoto, Y. M. Lee, W. Nam and S. Fukuzumi, *Inorg. Chem.* **2014**, *53*, 3618.
- (a) P. Leeladee, R. A. Baglia, K. A. Prokop, R. Latifi, S. P. de Visser and D. P. Goldberg, *J. Am. Chem. Soc.* **2012**, *134*, 10397; (b) R. A. Baglia, M. Dürr, I. Ivanović-Burmazović and D. P. Goldberg, *Inorg. Chem.* **2014**, *53*, 5893.
- S. Fukuzumi, Y. Morimoto, H. Kotani, P. Naumov, Y. M. Lee and W. Nam, *Nat. Chem.* **2010**, *2*, 756.
- Y. J. Park, S. A. Cook, N. S. Sickerman, Y. Sano, J. W. Ziller and A. S. Borovik, *Chem. Sci.* **2013**, *4*, 717; (b) Y. J. Park, J. W. Ziller and A. S. Borovik, *J. Am. Chem. Soc.* **2011**, *133*, 9258.
- Z. Zhang, K. L. Coats, Z. Chen, T. J. Hubin and G. Yin, *Inorg. Chem.* **2014**, *53*, 11937.
- F. Li, K. M. van Heuvelen, K. K. Meier, E. Münck and L. Que Jr. *J. Am. Chem. Soc.* **2013**, *135*, 10198.
- Y. Nishida, Y. M. Lee, W. Nam and S. Fukuzumi, *J. Am. Chem. Soc.* **2014**, *136*, 8042.

21. (a) G. Yin, *Acc. Chem. Res.* **2013**, *46*, 483; (b) Y. Wang, J. Sheng, S. Shi, D. Zhu and G. Yin, *J. Phys. Chem. C* **2012**, *116*, 13231; (c) S. Shi, Y. Wang, A. Xu, H. Wang, D. Zhu, S. B. Roy, T. A. Jackson, D. H. Busch and G. Yin, *Angew. Chem., Int. Ed.* **2011**, *50*, 7321; (d) A. Xu, H. Xiong and G. Yin, *Chem.-Eur. J.* **2009**, *15*, 11478; (e) Y. Wang, S. Shi, H. Wang, D. Zhu and G. Yin, *Chem. Commun.* **2012**, *48*, 7832; (f) G. Yin, A. M. Danby, D. Kitko, J. D. Carter, W. M. Scheper and D. H. Busch, *Inorg. Chem.* **2007**, *46*, 2173; (g) G. Yin, A. M. Danby, D. Kitko, J. D. Carter, W. M. Scheper and D. H. Busch, *J. Am. Chem. Soc.* **2008**, *130*, 16245.
22. H. Guo, Z. Chen, F. Mei, D. Zhu, H. Xiong and G. Yin, *Chem.-Asian. J.* **2013**, *8*, 888.
23. (a) L. Dong, Y. Wang, Y. Lv, Z. Chen, F. Mei, H. Xiong and G. Yin, *Inorg. Chem.* **2013**, *52*, 5418; (b) Z. Chen, L. Yang, C. Choe, Z. Lv and G. Yin, *Chem. Comm.* **2015**, *51*, 1874.
24. Z. Tyeklár, R. R. Jacobson, N. Wei, N. N. Murthy, J. Zubieta and K. D. Karlin, *J. Am. Chem. Soc.* **1993**, *115*, 2677.
25. T. Kojima, R. A. Leising, S. Yan and L., Que Jr. *J. Am. Chem. Soc.* **1993**, *115*, 11328.
26. D. Mandon, A. Machkour, S. Goetz and R. Welter, *Inorg. Chem.* **2002**, *41*, 5364.
27. A. Diebold and K. S. Hagen, *Inorg. Chem.* **1998**, *37*, 215.
28. (a) F. P. Guengerich, *Chem. Res. Toxicol.* **2001**, *14*, 611; (b) C. L. Shaffer, S. Harriman, Y. M. Koen and R. P. Hanzlik, *J. Am. Chem. Soc.* **2002**, *124*, 8268; (c) S. B. Karki, J. P. Dinnocenzo, J. P. Jones and K. P. Korzekwa, *J. Am. Chem. Soc.* **1995**, *117*, 3657; (d) C. Li, W. Wu, K. B. Cho and S. Shaik, *Chem.-Eur. J.* **2009**, *15*, 8492; (e) F. P. Guengerich, C. H. Yun and T. L. Macdonald, *J. Biol. Chem.* **1996**, *271*, 27321; (f) M. N. Bhakta and K. Wimalasena, *J. Am. Chem. Soc.* **2002**, *124*, 1844; (g) A. G. Roberts, S. E. A. Sjögren, N. Fomina, K. T. Vu, A. Almutairi and J. R. Halpert, *Biochem.* **2011**, *50*, 2123; (h) G. Galliani and B. Rindone, *J. Chem. Soc., Perkin. Trans.* **1978**, *5*, 456; (i) C. L. Shaffer, M. D. Morton and R. P. Hanzlik, *J. Am. Chem. Soc.* **2001**, *123*, 8502; (j) G. T. Miwa and J. S. Walsh, *J. Biol. Chem.* **1983**, *258*, 14445; (k) P. F. Hollenberg, *FASEB. J.* **1992**, *6*, 686; (l) K. Wimalasena and S. W. May, *J. Am. Chem. Soc.* **1987**, *109*, 4036.
29. (a) D. Bahulayan, R. Sukumar, K. R. Sabu and M. Lalithambika, *Green. Chem.* **1999**, *1*, 191; (b) H. Takahashi, N. Kashiwa, Y. Hashimoto and K. Nagasawa, *Tetrahedron. Lett.* **2002**, *43*, 2935.
30. (a) J. Park, Y. Morimoto, Y. M. Lee, Y. You, W. Nam and S. Fukuzumi, *Inorg. Chem.* **2011**, *50*, 11612; (b) M. Kirchgessner, K. Sreenath and K. R. Gopidas, *J. Org. Chem.* **2006**, *71*, 9849.
31. J. G. López-Cortés, G. Penieres-Carrillo, M. C. Ortega-Alfaro, R. Gutiérrez-Pérez, R. A. Toscano and C. Alvarez-Toledano, *Can. J. Chem.* **2000**, *10*, 1299.
32. (a) C. G. Hover and A. P. Kulkarni, *Chem-Biol. Inter.* **2000**, *124*, 191; (b) R. Hand and R. F. Nelson, *J. Electrochem. Soc.* **1970**, *117*, 1353; (c) S. Murata, M. Miura and M. Nomura, *J. Chem. Soc., Chem. Commun.* **1989**, *2*, 116.
33. H. Yoon, Y. Morimoto, Y. M. Lee, W. Nam and S. Fukuzumi, *Chem. Commun.* **2012**, *48*, 11187.
34. (a) R. E. Childs and W. G. Bardsley, *Biochem. J.* **1975**, *145*, 93; (b) S. L. Scott, W. J. Chen, A. Bakac and J. H. Espenson, *J. Phys. Chem.* **1993**, *97*, 6710; (c) J. L. Zhang, D. K. Garner, L. Liang, D. A. Barrios and Y. Lu, *Chem.-Eur. J.* **2009**, *15*, 7481; (d) R. Re, N. Pellegrini, A. Proteggente, A. Pannala, M. Yang and C. Rice-Evans, *Free. Radical. Bio. Med.* **1999**, *26*, 1231.
35. (a) J. U. Rohde, J. H. In, M. H. Lim, W. W. Brennessel, M. R. Bukowski, A. Stubna, E. Münck, W. Nam and L. Que Jr. *Science*, **2003**, *299*, 1037; (b) J. U. Rohde, A. Stubna, E. L. Bominaar, E. Münck, W. Nam and L. Que Jr. *Inorg. Chem.* **2006**, *45*, 6435; (c) A. T. Fiedler and L. Que Jr. *Inorg. Chem.* **2009**, *48*, 11038; (d) C. Krebs, D. G. Fujimori, C. T. Walsh and J. M. Bollinger Jr. *Acc. Chem. Res.* **2007**, *40*, 484; (e) K. Chen, M. Costas and L. Que Jr. *J. Chem. Soc., Dalton Trans.* **2002**, *5*, 672; (f) K. Ray, J. England, A. T. Fiedler, M. Martinho, E. Münck and L. Que Jr. *Angew. Chem., Int. Ed.* **2008**, *47*, 8068.
36. (a) S. C. Trewick, T. F. Henshaw, R. P. Hausinger, T. Lindahl and B. Sedgwick, *Nature* **2002**, *419*, 174; (b) P. Ø. Falnes, R. F. Johansen and E. Seeberg, *Nature* **2002**, *419*, 178; (c) M. Camps, B. F. Eichman and *Molecular. Cell.* **2011**, *44*, 343; (d) C. Zhu, C. Yi and *Angew. Chem., Int. Ed.* **2014**, *53*, 3659.
37. M. H. Lim, J. U. Rohde, A. Stubna, M. R. Bukowski, M. Costas, R. Y. N. Ho, E. Münck, W. Nam and L. Que Jr. *P Natl. Acad. Sci. USA*, **2003**, *100*, 3665.
38. (a) C. R. Goldsmith and P. T. D. Stack, *Inorg. Chem.* **2006**, *45*, 6048; (b) J. P. Roth and J. M. Mayer, *Inorg. Chem.* **1999**, *38*, 2760.
39. (a) G. J. P. Britovsek, J. England and A. J. P. White, *Inorg. Chem.* **2005**, *44*, 8125; (b) S. Furukawa, Y. Hitomi, T. Shishido and T. Tanaka, *Inorg. Chim. Acta.* **2011**, *378*, 19.
40. Y. Zang, J. Kim, Y. Dong, E. C. Wilkinson, E. H. Appelman and L. Que Jr. *J. Am. Chem. Soc.* **1997**, *119*, 4197.
41. (a) E. Skrzypczak-Jankun, R. A. Bross, R. T. Carroll, W. R. Dunham and M. O. Funk Jr. *J. Am. Chem. Soc.* **2001**, *123*, 10814; (b) T. R. Holman, J. Zhou and E. I. Solomon, *J. Am. Chem. Soc.* **1998**, *120*, 12564; (c) S. Ogo, R. Yamahara, M. Roach, T. Suenobu, M. Aki, T. Ogura, T. Kitagawa, H. Masuda, S. Fukuzumi and Y. Watanabe, *Inorg. Chem.* **2002**, *41*, 5513.
42. (a) J. P. Hage, J. R. Schnelten and D. T. Sawyer, *Bioorg. Med. Chem.* **1996**, *4*, 821; (b) B. Chiavarino, R. Cipollini, M. E. Crestoni, S. Fornarini, F. Lanucara and A. Lapi, *J. Am. Chem. Soc.* **2008**, *130*, 3208.
43. M. Finn, R. Friedline, N. K. Suleman, C. J. Wohl and J. M. Tanko, *J. Am. Chem. Soc.* **2004**, *126*, 7578.
44. S. Sumalekshmy and K. R. Gopidas, *Chem. Phys. Lett.* **2005**, *413*, 294.
45. J. Prakash, G. T. Rohde, K. K. Meier, A. J. Jasnowski, K. M. Van Heuvelen, E. Münck, and L. Que, Jr. *J. Am. Chem. Soc.* **2015**, *137*, 3478.

Table of contents

Interacting of Zn^{2+} with $\text{Fe}(\text{TPA})\text{Cl}_3$ can trigger ET from amine to iron(III) with generating substrate radical which traps dioxygen to produce alkylperoxyl, thus initiate catalytic oxidation, resembling lipoxygenase-like dioxygen activation.

